

A design scheme for interference suppression based on CWBIM^①

WANG Yunzhe (王蕴哲), MA Tianming^②, JIANG Xiaoxiao, MA Honglei
(School of Electrical and Electronic Engineering, Shanghai University of Engineering Science,
Shanghai 201620, P. R. China)

Abstract

An interference suppression design scheme based on conjugate weighted butterfly interleaving mapping (CWBIM) is proposed for inter-carrier interference (ICI) and inter-subband interference (IBI) in the received signals of universal filtered multi-carrier (UFMC) systems. It applies an interleaving mapping operation to subtract the interference coefficients of adjacent terms in ICI and IBI twice, thereby achieving suppression effects similar to the self-cancellation (SC) algorithm while maintaining the original data transmission efficiency. Meanwhile, conjugate and complex weighting operations can effectively suppress the impact of phase rotation errors in high-speed mobile channel environments, thereby further improving the bit error rate (BER) performance of the system. Moreover, butterfly operation can effectively control the computational complexity of the interleaving mapping process. Theoretical analysis and simulation results show that, compared with the PSC-UFMC algorithm, the CWBIM-UFMC scheme proposed in this paper can effectively suppress ICI and IBI in the received signal without compromising data transmission efficiency and reducing computational complexity, thereby achieving good BER performance of the system.

Key words: universal filtered multi-carrier (UFMC), inter-carrier interference (ICI), inter-subband interference (IBI), butterfly interleaving mapping

0 Introduction

Orthogonal frequency division multiplexing (OFDM) is widely used in the 4th-generation mobile communication technology (4G) because of its high frequency utilization and good anti-frequency selective fading characteristics. However, OFDM itself also has a large peak-to-average power ratio (PAPR), high out-of-band radiation, and is very sensitive to phase noise and carrier frequency offset (CFO) and other defects^[1]. To better support the performance challenges faced by multiple scenarios in 5th-generation mobile communication technology (5G), an effective solution is to optimize and improve existing technologies^[2]. As a result, filter bank multi-carrier (FBMC)^[3], general frequency division multiplexing (GFDM)^[4] and universal filtered multi-carrier (UFMC) have emerged as some new multi-carrier modulation techniques.

The UFMC technique was first proposed in Ref. [5]. Unlike FBMC which is filtered on a subcarrier basis, UFMC uses subband filtering, and the interference be-

tween adjacent subbands is reduced after filtering, making UFMC very robust^[6]. Therefore, it can not only avoid the shortcomings of OFDM such as poor out-of-band suppression performance and inability to support asynchronous transmission, but also overcome the shortcomings of FBMC such as poor compatibility with multiple-input multiple-output (MIMO) technology and unsuitability for short burst data transmission. However, the filtering characteristics of the UFMC dictate that the subcarriers within each subband still require overlapping orthogonal and synchronous transmission, and a certain amount of inter-subband interference (IBI) is generated between adjacent subbands^[7]. Therefore, how to effectively perform interference suppression is one of the current research hotspots of UFMC.

There is a lot of literature on OFDM interference suppression in China and abroad, but there is relatively little literature on UFMC interference suppression. Ref. [8] used the carrier frequency bias as well as the joint maximum likelihood estimation of the channel to predict the initial CFO and design the frequency domain equalizer u-

① Supported by the National Natural Science Foundation of China (No. 61601296, 61701295), the Science and Technology Innovation Action Plan Project of Shanghai Science and Technology Commission (No. 20511103500), and the Talent Program of Shanghai University of Engineering Science (No. 2018RC43).

② To whom correspondence should be addressed. E-mail: tmma@sues.edu.cn.
Received on May. 26, 2023

using the rotation concept, then iterative methods are used to find the true frequency, and finally the frequency domain equalizer is used to remove multipath interference. However, this method uses a rotational iterative search method to estimate the iterative step frequency when suppressing multipath interference, which leads to a large computational complexity. A linear weighting algorithm for inter-carrier interference (ICI) self-cancellation (SC) linear functions was proposed in Ref. [9], so that interference self-cancellation and linear weighting of first-order functions are combined to weight each subsequence with a linear product, ultimately reducing the ICI of the received signal, but the method requires a cyclic prefix and is not applicable in UFMC systems. Ref. [10] performed symbol time compression on OFDM symbols by tripling the subcarrier spacing in half the duration, thus reducing the normalized Doppler frequency by 50%, which enhances the ability to suppress ICI. In Ref. [11], the UFMC-AIC technique was proposed to obtain a higher transmission rate as well as better BER performance by inserting a predefined ICI interference cancellation algorithm between adjacent subbands and optimizing its weighting factor, but the complexity of the algorithm is large. Ref. [12] combined the idea of the SC algorithm in OFDM into UFMC (abbreviated as SC-UFMC) and proposed a partial interference cancellation (PSC) interference suppression algorithm (abbreviated as PSC-UFMC), but using the SC algorithm for the sequences at both ends of the signal will lead to some loss of data transmission efficiency, and the use of the windowing technique to suppress interference will inevitably cause some distortion and warping to the received signal itself^[13], which in turn affects the system BER performance.

To solve the problem of high interference in the UFMC, an interference suppression scheme based on conjugate weighted butterfly interleaving mapping (CWBIM) is proposed. In this paper, the signals transmitted in the UFMC system are derived through a process of mobile communication channels with time-varying and multipath effects, next the various interference components in the received signal are analyzed. Then, in response to the issue proposed in Ref. [12] that SC-UFMC and PSC-UFMC can lead to a decrease in data transmission efficiency, and the windowing technique in PSC-UFMC can cause signal distortion, CWBIM is proposed to address ICI and IBI in the received signal, but also overcome the shortcomings of reduced transmission efficiency and distortion of the received signal while improving the computational complexity less.

1 UFMC system model and interference analysis

The structure diagram of UFMC system is shown in Fig. 1.

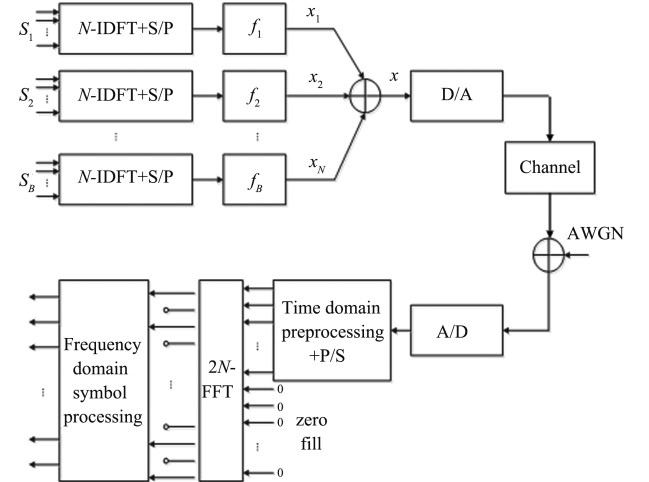


Fig. 1 The structure diagram of a UFMC system

For the sake of analysis, here assume a single-user scenario. First, at the transmitter side of the system, the N subcarriers in the UFMC are divided into B subbands, and the number of subcarriers in each subband is $N_B = N/B$. Suppose the transmitted signal on the k ($0 \leq k \leq N_B - 1$) subcarrier in subband i ($1 \leq i \leq B$) is $S_i(k)$, then it obtains the time domain signal $s_i(n)$ ($0 \leq n \leq N - 1$) after N -point inverse discrete Fourier transform (IDFT) ($0 \leq n \leq N - 1$) can be expressed as^[5]

$$s_i(n) = \frac{1}{N} \sum_{k=0}^{N_B-1} S_i(k) e^{j2\pi kn/N} \quad (1)$$

Subband filtering is then performed, and the filters in each subband can be the same or different. In the same way, it is assumed here that the filters are all identical. Assuming that the length of $f_i(n)$ is L , then the final transmit signal $x(n)$ ($0 \leq n \leq N + L - 1$) can be expressed as the superposition of the filtered time domain signals in all subbands:

$$\begin{aligned} x(n) &= \sum_{i=1}^B x_i(n) = \sum_{i=1}^B s_i(n) * f_i(n) \\ &= \sum_{i=1}^B \sum_{l=0}^{L-1} s_i(n) f_i(n-l) \\ &= \frac{1}{N} \sum_{i=1}^B \sum_{l=0}^{L-1} \sum_{k=0}^{N_B-1} S_i(k) f_i(n-l) e^{j2\pi kn/N} \quad (2) \end{aligned}$$

where, $f_i(n)$ denotes the filter in subband i , $x_i(n)$ is the signal obtained from $s_i(n)$ after filtering, and $*$ denotes the linear convolution operation.

When the transmitted signal is transmitted in the channel, considering the multipath effect as well as the CFO in the actual channel, the received signal $y(n)$ received at the receiving end can be expressed as

$$\begin{aligned} y(n) &= x(n) * h(n) e^{j2\pi n \varepsilon / N} + \omega(n) \\ &= \sum_{p=0}^{P-1} a_p x(n-p) e^{j2\pi n \varepsilon / N} + \omega(n) \end{aligned} \quad (3)$$

where, $h(n)$ is the channel impulse response with multipath effect; a_p and $p = \tau_p$ ($0 \leq p \leq P-1$, $\tau_0 \leq \tau_1 \leq \dots \leq \tau_{P-1}$) are the strength and arrival time of each signal, respectively; P is the number of all propagation paths; ε ($0 \leq \varepsilon \leq 1$) is normalized frequency offset (NFO); $\omega(n) \sim \mathcal{N}(0, \sigma^2)$ is additive white Gaussian noise (AWGN).

Then the $2N$ -point fast Fourier transform (FFT) is performed on $y(n)$. Since the length of $y(n)$ is also $N+L-1$ like $x(n)$, it is necessary to add $N-L+1$ zeros before performing the $2N$ -point FFT. The frequency domain signal $Y(m)$ ($0 \leq m \leq 2N-1$) after a $2N$ -point FFT can be expressed as

$$\begin{aligned} Y(m) &= \sum_{n=0}^{N+L-2} \left(\sum_{p=0}^{P-1} a_p x(n-p) e^{j2\pi n \varepsilon / N} + \omega(n) \right) e^{-j2\pi m n / 2N} \\ &= \sum_{i=1}^B \sum_{k=0}^{N_B-1} S_i(k) I_i(k-m) + W(m) \\ &= S_b(m) I_b(0) + \underbrace{\sum_{k=0, k \neq m}^{N_B-1} S_b(k) I_b(k-m)}_{\text{ICI}} \\ &\quad + \underbrace{\sum_{i=1, i \neq b}^B \sum_{k=0}^{N_B-1} S_i(k) I_i(k-m)}_{\text{IBI}} + W(m) \end{aligned} \quad (4)$$

where $W(m)$ is the frequency domain expression for $\omega(n)$, $I_b(0)$ is the useful signal coefficient, and $I_i(k-m)$ is the interference coefficient, which can be expressed as

$$I_i(k-m) = \frac{1}{N} \sum_{n=0}^{N+L-2} \sum_{l=0}^{L-1} \sum_{p=0}^{P-1} a_p f_i(n-p-l) \cdot e^{-j2\pi k p / N} e^{j2\pi \varepsilon (k-m/2 + \varepsilon) n / N} \quad (5)$$

It can be seen that when there is no frequency error in the system (i. e. $\varepsilon = 0$), $I_b(0)$ achieves the maximum value of 1. However, as ε increases, $I_b(0)$ will gradually decrease and $I_i(k-m)$ will gradually increase.

According to Eq. (4), it is easy to see that for a transmit signal $S_b(k)$ in a given subband b , the interference in $Y(m)$ contains IBI terms between different subbands as well as ICI terms within the same subband. Owing to $N_B = N/B < N$, the ICI terms of UFMC are usually much smaller than that in OFDM with the same N . In addition, considering the good compatibility

between UFMC and OFDM, the adjacent ICI in the same subband of $Y(m)$ also varies a little. Moreover, it is easy to find that the interference coefficients of the IBI terms in Eq. (4) are composed of $I_i(k-m)$, therefore the IBI between adjacent subbands in $Y(m)$ is also relatively approximate, the SC algorithm in OFDM can also be adopted in UFMC interference suppression.

2 CWBIM interference suppression scheme

In this section, a CWBIM-based interference suppression scheme is proposed, as shown in Fig. 2. The whole process can be divided into the following stages.

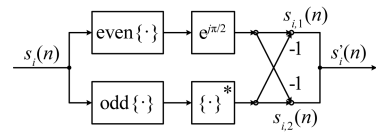


Fig. 2 The structure diagram of conjugate weighted butterfly interleaving mapping (CWBIM)

Firstly, $L(n)$ can be obtained by multiplying the even sequences of $s_i(n)$ by a complex weighting factor $e^{j\pi/2}$ and conjugating them to the odd sequences of $s_i(n)$, which can be formulated by

$$\begin{aligned} L(n) &= \begin{cases} e^{j\pi/2} \cdot \text{even}\{s_i(n)\} & n \text{ is even} \\ (\text{odd}\{s_i(n)\})^* & n \text{ is odd} \end{cases} \\ &= \begin{cases} e^{j\pi/2} s_i(n) & n \text{ is even} \\ s_i^*(n) & n \text{ is odd} \end{cases} \end{aligned} \quad (6)$$

where $\text{odd}\{\cdot\}$ and $\text{even}\{\cdot\}$ denote the odd and even part of the extracted sequences, respectively, and $(\cdot)^*$ represents finding conjugation for a sequence.

Secondly, $s_{i,1}(n)$ and $s_{i,2}(n)$ can be obtained by mapping the even and odd sequences of $L(n)$ by the following butterfly interleaving respectively, which can be depicted as

$$\begin{aligned} s_{i,1}(n) &= \begin{cases} L(n) & n \text{ is even} \\ -L(n) & n \text{ is odd} \end{cases} \\ &= \begin{cases} e^{j\pi/2} s_i(n) & n \text{ is even} \\ -s_i^*(n) & n \text{ is odd} \end{cases} \end{aligned} \quad (7)$$

$$\begin{aligned} s_{i,2}(n) &= \begin{cases} \text{odd}\{L(n)\} & n \text{ is even} \\ -\text{even}\{L(n)\} & n \text{ is odd} \end{cases} \\ &= \begin{cases} s_i^*(n+1) & n \text{ is even} \\ -e^{j\pi/2} s_i(n-1) & n \text{ is odd} \end{cases} \end{aligned} \quad (8)$$

Finally, the desired sequence signal $s'_i(n)$ can be given by merging and adding $s_{i,1}(n)$ and $s_{i,2}(n)$, that is

$$\begin{aligned} s'_i(n) &= s_{i,1}(n) + s_{i,2}(n) \\ &= \begin{cases} e^{j\pi/2} s_i(n) + s_i^*(n+1) & n \text{ is even} \\ e^{-j\pi/2} s_i(n-1) - s_i^*(n) & n \text{ is odd} \end{cases} \end{aligned} \quad (9)$$

According to the properties of discrete Fourier transform (DFT), it is easy to get;

$$e^{j\pi/2} s_i(n) + s_i^*(n+1) \xrightarrow{N/2 - \text{DFT}} S_i^*(-k) e^{j2\pi k/N} + jS_i(k) \quad (10)$$

$$e^{-j\pi/2} s_i(n-1) - s_i^*(n) \xrightarrow{N/2 - \text{DFT}} -S_i^*(-k) - jS_i(k) e^{-j2\pi k/N} \quad (11)$$

Therefore, if $s_i'(n)$ is applied as the time domain signal in subband i , then the frequency domain signal $Y'(m)$ and $Y'(m+1)$ on the m and $m+1$ subcarrier respectively after $2N$ -FFT can be expressed as

$$Y'(m) = \sum_{i=1}^B \sum_{k=0}^{N_B/2-1} [jS_i(k)(I_i(k-m) - I_i(k-m-1)) + S_i^*(-k)(I_i(k-m+1) - I_i(k-m))] + W(m) \quad (12)$$

$$Y'(m+1) = \sum_{i=1}^B \sum_{k=0}^{N_B/2-1} [jS_i(k)(I_i(k-m-1) - I_i(k-m-2)) + S_i^*(-k)(I_i(k-m) - I_i(k-m-1))] + W(m+1) \quad (13)$$

The final received sequence signal $Y''(m)$ can be achieved by subtracting $Y'(m)$ from $Y'(m+1)$, that is

$$Y''(m) = Y'(m+1) - Y'(m) = jS_b(m)(2I_b(-1) - I_b(0) - I_b(-2)) + S_b^*(-k)(2I_b(0) - I_b(-1) - I_b(1)) + \underbrace{\sum_{k=0, k \neq m}^{N_B/2-1} \left\{ jS_b(k)(2I_b(k-m-1) - I_b(k-m) - I_b(k-m-2)) + S_b^*(-k)(2I_b(k-m) - I_b(k-m-1) - I_b(k-m+1)) \right\}}_{\text{ICI}} + \underbrace{\sum_{i=1, i \neq b}^B \sum_{k=0}^{N_B/2-1} \left\{ jS_i(k)(2I_i(k-m-1) - I_i(k-m) - I_i(k-m-2)) + S_i^*(-k)(2I_i(k-m) - I_i(k-m-1) - I_i(k-m+1)) \right\}}_{\text{IBI}} + W(m+1) - W(m) \quad (14)$$

According to Eq. (14), it is not difficult to see that the proposed CWBIM interference suppression scheme has the following advantages.

Firstly, similar to the SC algorithm in OFDM, CWBIM adopts the idea of interleaving mapping, which significantly eliminates the ICI and IBI terms in $Y''(m)$ by subtracting the difference between two adjacent interference coefficients $I_i(k-m)$ twice to achieve a good interference suppression effect.

Secondly, SC (or PSC) algorithm is self-modulated mapping for all (or part) of the sequences in the received signals, which will inevitably reduce the data transmission efficiency by half. Fortunately, the interleaving mapping operation in CWBIM can inhibit ICI and IBI while keeping the data transmission efficiency of original signals unchanged.

Thirdly, according to Eq. (9), CWBIM adopts operations such as conjugate calculation and multiplication of complex weighting factors to ensure that each term in $s_i'(n)$ contains a complex weighting factor and a conjugate component, so that the influence of phase rotation error caused by the received signal in the high-speed mobile channel environment can be suppressed effectively to further improve the BER performance of the system.

Finally, CWBIM draws on the idea of butterfly operation in FFT^[14], therefore, the computation amount of the entire interleaved mapping process is limited.

3 Simulation results and algorithm complexity analysis

In this section, performance simulation and complexity analysis are performed for CWBIM-UFMC interference suppression scheme with conventional UFMC, SC-UFMC, and PSC-UFMC mentioned in Ref. [12]. The simulation parameters are shown in Table 1. Given that the actual 5G communication channel usually has both multipath and Doppler effects, ITU-VB is selected as the simulated channel model^[15], and its power delay distribution parameters^[13] are shown in Table 2. The degree of multipath and Doppler effects in the channel is adjusted by adjusting the number of propagation paths P in the channel and the normalized frequency bias ε . Assuming that the effect of ε is the same on each path.

Table 1 System simulation parameters

Parameters	Values/Explanations
Bandwidth	8 MHz
Modulation	QPSK, 16QAM
Number of subcarriers (N)	128
Number of subbands (B)	4, 8
Prototype filters	Dolph-Chebyshev
Filter lengths (L)	10
Number of propagation paths (P)	3, 6
Channel model	ITU-VB
Normalized frequency offset (ε)	0.1, 0.5
Noise model	AWGN

Table 2 Power delay distribution parameters of ITU-VB

Number of propagation paths (P)	ITU-VB	
	Relative delay / μs	Average power / dB
1	0.0	-2.5
2	0.3	0.0
3	8.9	-12.8
4	12.9	-10.0
5	17.1	-25.2
6	20.0	-16.0

Firstly, the performance of interference suppression is analyzed. The proportion of interference in the overall received signal can be measured by carrier in-

terference ratio (CIR), which can be expressed as^[16]

$$CIR \triangleq \frac{E[|C(m)|^2]}{E[|I(m)|^2]} \quad (15)$$

where $E[|C(m)|^2]$ and $E[|I(m)|^2]$ are the carrier power and the interference power of the received signal respectively. According to Eq. (4), Ref. [12], and Eq. (14), it is not difficult to derive the CIR of conventional UPMC, SC-UPMC, PSC-UPMC, and CWBIM-UPMC at $m=0$ respectively as

$$CIR_{\text{original}} = \frac{|I_b(0)|^2}{\sum_{k=1}^{N_B-1} |I_b(k)|^2 + \sum_{i=1, i \neq b}^B \sum_{k=0}^{N_B-1} |I_i(k)|^2} \quad (16)$$

$$CIR_{\text{SC}} = \frac{|2I_b(0) - I_b(-1) - I_b(1)|^2}{\sum_{k=1}^{N_B-1} |2I_b(k) - I_b(k-1) - I_b(k+1)|^2 + \sum_{i=1, i \neq b}^B \sum_{k=0}^{N_B-1} |2I_i(k) - I_i(k-1) - I_i(k+1)|^2} \quad (17)$$

$$CIR_{\text{PSC}} = \begin{cases} \frac{|2I_b(0) - I_b(-1) - I_b(1)|^2}{\sum_{k=2}^{N_B-1} |2I_b(k) - I_b(k-1) - I_b(k+1)|^2 + \sum_{i=1, i \neq b, k=0, k=\text{even}}^B \sum_{k=0}^{N_B-1} |2I_i(k) - I_i(k-1) - I_i(k+1)|^2} & k \in \{0, 2, N_B - 4, N_B - 2\} \\ \frac{|I_b(0)|^2}{\sum_{k=1}^{N_B-1} |I_b(k)|^2 + \sum_{i=1, i \neq b}^B \sum_{k=0}^{N_B-1} |I_i(k)|^2} & k \in \{3, N_B - 5\} \end{cases} \quad (18)$$

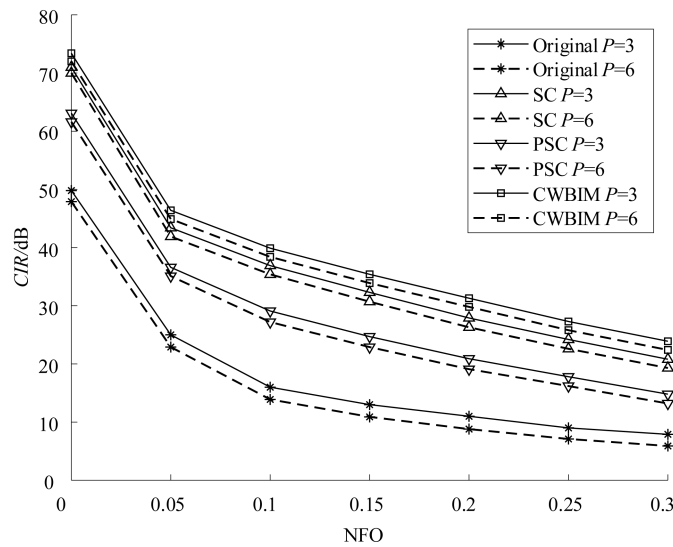
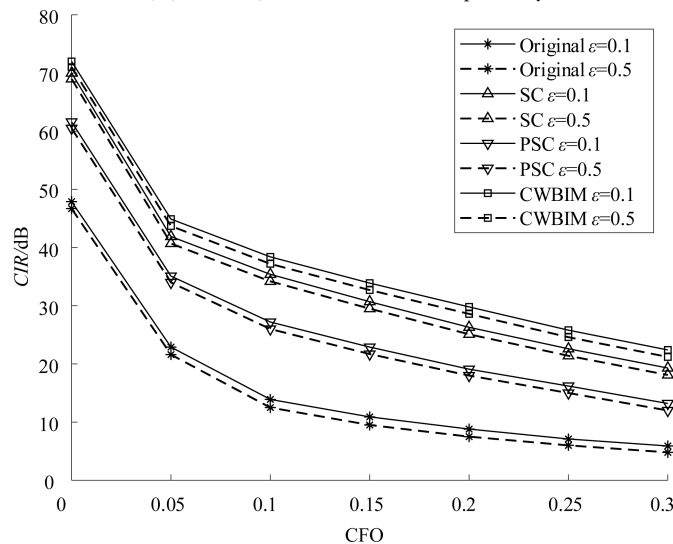
$$CIR_{\text{CWBIM}} = \frac{|2I_b(-1) - I_b(0) - I_b(-2)|^2 + |2I_b(0) - I_b(-1) - I_b(1)|^2}{\left\{ \sum_{k=1}^{N_B-1} [|2I_b(k-1) - I_b(k) - I_b(k-2)|^2 + |2I_b(k) - I_b(k-1) - I_b(k+1)|^2] + \sum_{i=1, i \neq b}^B \sum_{k=0}^{N_B-1} [|2I_i(k-1) - I_i(k) - I_i(k-2)|^2 + |2I_i(k) - I_i(k-1) - I_i(k+1)|^2] \right\}} \quad (19)$$

The method of variable control is applied to analyze the impact of P and ε respectively on CIR performance of various interference suppression schemes with QPSK modulation and $B=4$. The simulation results are demonstrated in Fig. 3, from which the following conclusions can be made.

(1) Fig. 3 shows the CIR plots of the above four suppression schemes with $\varepsilon=0.1$ and $P=3, 6$. From Fig. 3(a), it is easy to find that the interference suppression performance of all schemes deteriorates with the increase of P , which indicates that the multipath effect indeed affects the interference. It can also be seen that the CIR of SC is significantly better than that

of PSC, while the performance of CWBIM is slightly better than that of SC under the same P . This is because PSC adopts the windowing operation to reduce the loss of data transmission efficiency, resulting in significantly inferior interference suppression effect compared with SC. On the other hand, CWBIM performs interweaving mapping on the two sequences that have undergone conjugate and complex weighting operations respectively, thus further enhancing its ability to resist multipath effects compared with SC.

(2) Fig. 3(b) demonstrates the CIR curve of the above four suppression schemes with $P=3$ and $\varepsilon=0.1, 0.5$. According to Fig. 3(b), it can be seen that

(a) $\varepsilon = 0.1$, P takes 3 and 6 respectively(b) $P=6$, ε takes 0.1 and 0.5 respectively**Fig. 3** The CIR performance of different schemes with QPSK modulation and $B=4$

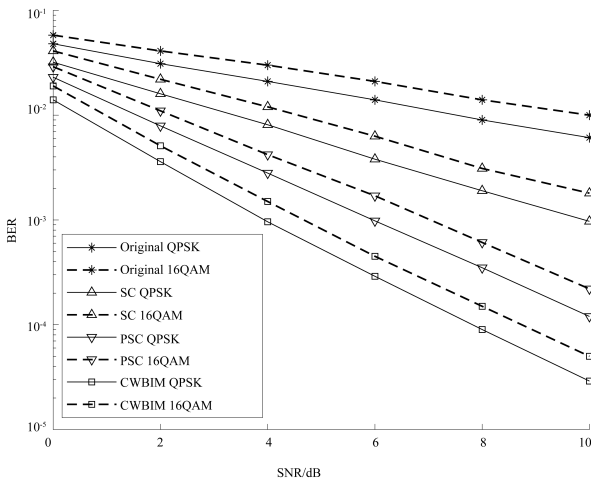
the performance of CIR also deteriorates by the increase of ε but the effect is not as obvious as that of P . This is because the effect of P on the interference coefficient $I_i(k-m)$ is larger than that of ε . It is also not difficult to discover that CWBIM displays the best CIR performance. Its primary reason lies in the fact that the conjugate and complex weighting operations weaken the effect of the phase rotation error caused by ε in the wireless channel to some extent.

Secondly, the performance of BER is simulated and analyzed. Similarly, the method of variable control is applied to analyze the impact of modulation modes, B , P , and ε respectively on the BER performance of various interference suppression schemes, which can be given in Fig. 4. From the results, it is not difficult to discover the following conclusions.

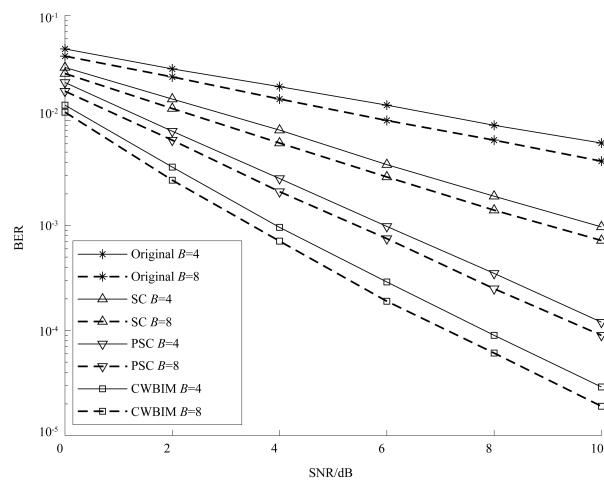
(1) Fig. 4 (a) shows the BER plots of the above

four suppression schemes with QPSK and 16QAM modulation respectively ($B=4$, $P=6$, $\varepsilon=0.1$). According to Fig. 4 (a), it is easy to conclude that applying different modulation modes can have a certain impact on the performance of the system. Meanwhile, the BER curves under QPSK are better than that of 16QAM, because of the superior fault tolerance. Given the complex characteristics of time-varying multipath fading channels, QPSK is more applied in most cases.

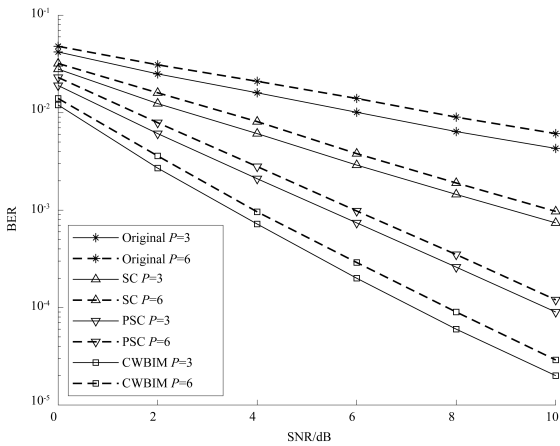
(2) Fig. 4 (b) depicts the BER plots of the above four suppression schemes with QPSK ($P=6$, $\varepsilon=0.1$, and $B=4, 8$). From Fig. 4 (b), it is not difficult to discover that the BER performance of the system improves with the increase of B when all other conditions are the same. This is due to the fact that an increase in B can further reduce the orthogonality requirement between subcarriers in the subband and improves the



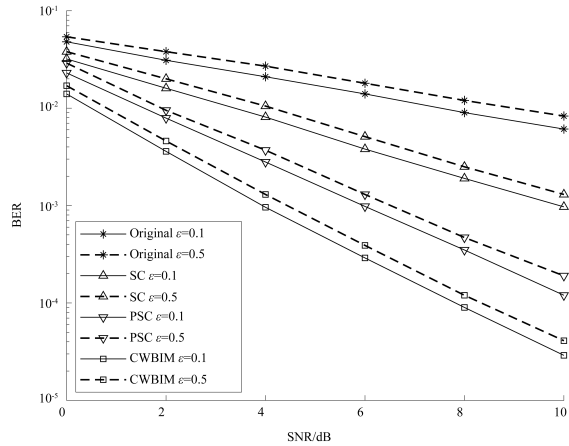
(a) $B = 4, P = 6, \varepsilon = 0.1$, the modulation methods are QPSK and 16QAM respectively



(b) QPSK modulation, $P = 6, \varepsilon = 0.1$, B takes 4 and 8 respectively



(c) QPSK modulation, $B = 4, \varepsilon = 0.1$, P takes 3 and 6 respectively



(d) QPSK modulation, $B = 4, P = 6, \varepsilon$ takes 0.1 and 0.5 respectively

Fig. 4 The BER performance of different schemes

out-of-band rejection performance of the system. However, the increase in B also leads to an increase in the complexity at the transmitter, therefore $B = 4$ is more appropriate.

(3) Fig. 4 (c) demonstrates the BER plots of the above four suppression schemes with QPSK modulation, ($B = 4, \varepsilon = 0.1$, and $P = 3, 6$). According to Fig. 4(c), it is easy to find that the performance of the system deteriorates with the increase of P due to the multipath effect, and different SNR would correspond to different BER values when the rest of conditions are the same and different P values lead to the change of Doppler frequency shift. And it can be found that the proposed scheme in this paper has a better performance with a relatively small degradation of BER performance due to the increase of P in the system, mainly because the dual-path interaction mapping effect is equivalent to a diversity effect that enhances the ability to combat multipath effects in the environment.

(4) Fig. 4(d) describes the BER plots for the above four suppression schemes with QPSK modulation, $B = 4, p = 6$, and $\varepsilon = 0.1, 0.5$. From Fig. 4(d), it can be seen that the BER performance of the system deteriorates as ε increases. The change of Doppler shift in the high mobile channel leads to the change of the signal, which will eventually lead to the change of ε and affect the BER performance of the system. The effect of ε on CIR has been analyzed before, and again, the larger ε is, the higher the degradation of system performance, the more interference in the system, and the worse the BER performance. The proposed scheme in this paper has better BER performance mainly because the presence of conjugate and complex weighting factors in the subcarriers can exhibit better system improvement due to carrier phase rotation.

Finally, the complexity of different schemes is compared and analyzed. The improvement of algorithm complexity is usually measured by the computational

complexity reduction ratio (CCRR), which can be defined by^[17]

$$\begin{aligned} CCRR &\triangleq \left(1 - \frac{\text{Complexity of new algorithm}}{\text{Complexity of the original algorithm}}\right) \\ &\times 100\% = \left(1 - \frac{\text{Complexity of CWBIM - UFMC}}{\text{Complexity of PSC - UFMC}}\right) \\ &\times 100\% \end{aligned} \quad (20)$$

The complexity of SC-UFMC is reflected by multiplying half of the transmit sequence by -1 , performing $2N$ -FFT at the receiver, and subtracting all adjacent subcarriers. From Ref. [13], it is known that the $2N$ -FFT requires $N \log_2 2N$ multiplication operations as well as $2N \log_2 2N$ addition operations. Therefore, its multiplicative complexity C_{RM_SC} and additive complexity C_{RA_SC} can be shown as

$$C_{RM_SC} = \frac{N}{2} + N \log_2 2N \quad (21)$$

$$C_{RA_SC} = 2N + 2N \log_2 2N \quad (22)$$

The computational effort of PSC-UFMC is reflected by multiplying the two transmit sequences by -1 , multiplying the sequences by the window function at the receiver side, performing $2N$ -FFT at the receiver, and subtracting the four sets of adjacent subcarriers. Thus its multiplication complexity C_{RM_PSC} and addition complexity C_{RA_PSC} can be given as

$$C_{RM_PSC} = N + L + 1 + N \log_2 2N \quad (23)$$

$$C_{RA_PSC} = 4 + 2N \log_2 2N \quad (24)$$

The computational effort of CWBIM-UFMC is reflected by multiplying half of the transmit sequence by a weighting factor, performing butterfly interleaving mapping followed by bitwise merge summation, $2N$ -FFT at the receiver, and subtracting all adjacent subcarriers. Thus its multiplication complexity C_{RM_CWBIM} and addition complexity C_{RA_CWBIM} can be formulated as

$$C_{RM_CWBIM} = \frac{3N}{2} + N \log_2 2N \quad (25)$$

$$C_{RA_CWBIM} = 3N + 2N \log_2 2N \quad (26)$$

When $N = 128$ and $L = 10$, the computational complexity and CCRR of the above interference suppression schemes are shown in Table 3. It is easy to see that the computational complexity of CWBIM-UFMC has a small increase compared with PSC-UFMC.

Table 3 The computational complexity and CCRR of different schemes with $N = 128$ and $L = 10$

	Multiplication	Additive
SC-UFMC	1 088	2 304
PSC-UFMC	1 163	2 052
CWBIM-UFMC	1 216	2 432
CCRR/%	-4.55	-18.52

4 Conclusions

In this paper, the received signal of UFMC systems is analyzed and a CWBIM-UFMC interference suppression scheme is proposed, which can effectively suppress ICI and IBI in the received signal by butterfly interleaving mapping with a small increase in computational complexity, while the data transmission efficiency is improved. Theoretical analysis and simulation results indicate that, compared with PSC-UFMC algorithm in the subband^[12], CWBIM-UFMC obtains better results in the aspects of interference suppression and BER performance only with a limited increase in computational complexity, which is promising for practical applications.

References

- [1] CAI Y, QIN Z, CUI F, et al. Modulation and multiple access for 5G networks [J]. IEEE Communications Surveys and Tutorials, 2018, 20(1): 629-646.
- [2] KUMAR V, MUKHERJEE M, LLORET J, et al. A joint filter and spectrum shifting architecture for low complexity flexible UFMC in 5G [J]. IEEE Transactions on Wireless Communications, 2021, 20(10): 6706-6714.
- [3] CHEN D, LAN J, LUO K, et al. Symbol encryption and placement design for OQAM/FBMC systems [J]. IEEE Transactions on Communications, 2022, 70(1): 552-563.
- [4] LIU Y, ZHU X, LIM E G, et al. A semi-blind multiuser SIMO GFDM system in the presence of CFOs and IQ imbalances [J]. IEEE Transactions on Wireless Communications, 2022, 21(1): 48-63.
- [5] VAKILIAN V, WILD T, SCHAICH F, et al. Universal-filtered multi-carrier technique for wireless systems beyond LTE [C] // Globecom Workshops. Atlanta, USA: IEEE, 2013: 223-228.
- [6] KONGARA G, HE C W, YANG L, et al. A comparison of CP-OFDM, PCC-OFDM and UFMC for 5G uplink communications [J]. IEEE Access, 2019, 7: 157574-157594.
- [7] WU L, ZHANG Z C, DANG J, et al. UFMC-based interference management for heterogeneous small-cell networks [J]. IEEE Access, 2019, 7: 136559-136567.
- [8] CHIU S H, FU K C, CHEN Y F. A modified algorithm for joint frequency offset and channel estimation in OFDM systems [C] // 2013 IEEE/CIC International Conference on Communications in China. Xi'an, China: IEEE, 2013: 327-332.
- [9] MA H, XU Y. Research on inter-carrier interference elimination algorithms in high-speed railway scenarios [C] // The 12th International Conference on Measuring Technology and Mechatronics Automation. Phuket, Thailand: IC-MTMA, 2020: 615-619.
- [10] EIBAKRY M S, EISHENAWY H A, AMMARA EHA. A symbol time compression for ICI reduction in high mobility OFDM systems [C] // The 29th International Conference on Microelectronics. Beirut, Lebanon: IEEE, 2017:

- 1-10.
- [11] WAGH H, ZHANG Z, ZHANG Y, et al. Enhanced inter-sub-band interference suppression for universal filtered multi-carrier transmission [C] // IEEE Wireless Communications and Networking Conference. San Francisco, USA: IEEE, 2017: 1-6.
- [12] LONG K, CHEN H, DUAN S, et al. Improved algorithm of carrier interference suppression in UFMC system [J]. *Application Research of Computers*, 2019, 36 (9): 2743-2745, 2749. (In Chinese)
- [13] LI L. Principles, applications, and simulations of MIMO-OFDM systems [M]. Beijing: China Machine Press, 2014: 27-29. (In Chinese)
- [14] LIANG Y, SUN W, ZHANG W. Fast Fourier transform architecture based on serial butterfly unit [J]. *Acta Scientiarum Naturalium Universitatis Nankaiensis*, 2021, 54 (5): 48-52. (In Chinese)
- [15] Recommendation. ITU-R M 1225. Guidelines for evaluation of radio transmission technologies for IMT-2000 [S]. Geneva, Switzerland: International Telecommunication Union, 1997.
- [16] SINGH P, SAHU O P. An overview of ICI self cancellation techniques in OFDM systems [C] // 2015 IEEE International Conference on Computational Intelligence & Communication Technology. Ghaziaba, India: IEEE, 2015: 299-302.
- [17] CHEN H, CHUNG K. A low complexity PTS technique using minimal trellis in OFDM systems [J]. *IEEE Transactions on Vehicular Technology*, 2018, 67 (1): 817-821.

WANG Yunzhe, born in 1997. He is an M. S. candidate at Shanghai University of Engineering Science. He received his B. S. degree from Henan Agricultural University in 2019. His research interests include UFMC communication technology and interference suppression.